ISSN 0022-4766, Journal of Structural Chemistry, 2022, Vol. 63, No. 2, pp. 293-301. © Pleiades Publishing, Ltd., 2022, corrected publication 2022.
Russian Text © The Author(s), 2022, published in Zhurnal Strukturnoi Khimii, 2022, Vol. 63, No. 2, pp. 224-232.

THEORETICAL ANALYSIS OF CATION-MIGRATION PATHS IN MICROPOROUS HETEROPHYLLOSILICATES WITH ASTROPHYLLITE AND VEBLENITE TYPE STRUCTURES

S. M. Aksenov[1]*, N. A. Yamnova[2], N. V. Chukanov[2,3], N. A. Kabanova[1,4], E. A. Kobeleva[2], D. V. Deyneko[2], and S. V. Krivovichev[1,5]

Framework titanosilicates of the heterophyllosilicate family with three-layer *HOH* modules have a microporous structure and are characterized by the occurrence of systems of wide intersecting or parallel channels. The theoretical analysis of possible migration paths of various cations is performed using the ToposPro program. It is found that in heterophyllosilicates with astrophyllite-1*A*/-2*M* and veblenite structure types, a one-dimensional conductivity of alkali metal ions (Na^+, K^+, Rb^+, Cs^+), silver (Ag^+), and lead (Pb^{2+}) is possible through a system of wide parallel channels in the [100] direction. Lithium substitution for large alkali cations appreciably changes the character of the ionic conductivity. Due to a smaller radius, Li^+ cations can pass through a window between channels, forming a two-dimensional conductive layer parallel to (001).

DOI: 10.1134/S002247662202010X

Keywords: heterophyllosilicates, astrophyllite, veblenite, ion-exchange, topology, Voronoi-Dirichlet polyhedra, cation migration.

INTRODUCTION

Natural and synthetic titanosilicates are of interest as promising materials having a wide spectrum of physical and chemical properties [1]. Layered, pseudo-layered, and framework titanosilicates with systems of wide channels are characterized by sorption [2] and ion-exchange properties [3-9]. The crystalline materials with framework structures containing systems of intersecting channels of different diameters usually exhibit ion-exchange properties [10]. During the ion exchange in these crystals, incoming and outgoing ions move in different channels, these processes occurring simultaneously, according to the conservation requirement of electroneutrality of the crystal. **In counter flows**, ion exchange is usually sterically hindered.

[1]Federal Research Center "Kola Scientific Center", Russian Academy of Sciences, Apatity, Russia; *aks.crys@gmail.com. [2]Lomonosov Moscow State University, Moscow, Russia. [3]Institute of Problems of Chemical Physics, Russian Academy of Sciences, Chernogolovka, Russia. [4]Samara State University, Samara, Russia. [5]St. Petersburg State University, St. Petersburg, Russia. Original article submitted March 13, 2021; revised August 11, 2021; accepted September 14, 2021.

Framework titanosilicates of the heterophyllosilicate family [6, 11-13], whose structures are based on three-layer *HOH* modules, where the central *O*-layer is formed by edge-sharing *M*-octahedra and external *H*-layers are represented by a network of SiO_4 tetrahedra and Tiφ$_6$ octahedra (or Tiφ$_5$ semi-octahedra), possess a microporous structure and are characterized by the occurrence of systems of wide intersecting (perrotite group) or parallel channels (astrophyllite supergroup, nafertisite group, veblenite). From the experimental data and theoretical calculations it was previously found [14] that in mineral caryochroite (nafertisite structure type), ion exchange is possible in counter flows for Na^+, K^+, Rb^+, Cs^+, Ag^+, and Pb^{2+} ions, and for lithium ions possible exchange between the neighboring channels with the formation of two-dimensional conductivity, was also established.

The astrophyllite supergroup is formed by minerals with the general formula $A_{2p}B_rC_7D_2(Si_4O_{12})_2IX^O_{D2}X^O_{A4}X^P_{Dn}W_{A2}$, where C = Fe^{2+}, Mn, Na, Mg, Zn, Fe^{3+}, Ca, Zr, Li are the cations located in *M*-sites of the octahedral *O*-layer; $^{[6,5]}D$ = Ti, Nb, Zr, Sn^{4+}, $^{[5]}Fe^{3+}$, Mg, Al are the cations located in *L*-sites of the heteropolyhedral *H*-layer; A = K, Cs, Ba, H_2O, Li, Pb^{2+}, Na, □; p = 1, 2; B = Na, Ca, Ba, H_2O, □; r = 1, 2; X^O_D = O; X^O_A = OH, F; X^P_{Dn} = O, OH, F, H_2O, □; n = 0, 1, 2; W_A=H_2O, □; I (in the devitoite structure) = $(PO_4)_2(CO_3)$ [15]. This supergroup combines triclinic and monoclinic minerals [15-17] of the heterophyllosilicate family, which are characterized by a high degree of silicon polymerization expressed by the presence of wide tetrahedral ribbons Si_4O_{12}. Titanium atoms are in the octahedral coordination (being involved in the combination of neighboring *HOH* modules into a heteropolyhedral quasi-framework through common oxygen vertices) and in the semi-octahedral (tetragonal-pyramidal) coordination. Using the structure generation function $S_{N.n}$ [13], the general formula of the astrophyllite *HOH* module can be written as

$$(HOH)_{(Astro)} = \{^{[6]}M_7\varnothing_4[^{[5\text{-}6]}LO(Si_4O_{12})\Theta_n]_2\},$$

where *M* are cations of the octahedral *O*-layer; ∅-ligands (X^O_A-anions) belong to the octahedral *O*-layer, and Θ-ligands (X^P_D-anions) are apical (n = 1) or bridging (n = 0.5) vertices of *L*φ$_6$ octahedra of the neighboring *HOH* modules (in the case of *L*O$_5$ semi-octahedra, n = 0). A negative charge of the astrophyllite *HOH* module is compensated by alkali and alkaline earth *A*-cations located, along with water molecules, either in the interlayer space (in the case of isolated *HOH* modules) or wide channels stretched in the [100] direction (in the case of the combination of neighboring *HOH* modules).

With regard to different coordinations of titanium, and also possible ways of combining *HOH* modules (straight through the vertices of Tiφ$_6$ octahedra), four structure types may be distinguished for minerals of the astrophyllite group [15-19].

1. The astrophyllite structure type in which *HOH* modules are combined via bridging Θ-ligands of *L*φ$_6$ octahedra (n = 0.5). This structure type can have two polytypes that differ in combination features of the neighboring *HOH* modules, and consequently, symmetry and unit cell parameters [20]:

a) triclinic 1*A*-polytype (a ~ 5.4 Å, b ~ 11.9 Å, c ~ 11.7 Å, α ~ 113.0°, β ~ 94.5°, γ ~ 103.1°; space group $P\bar{1}$) (Fig. 1*a*);

b) monoclinic 2*M*-polytype (a ~ 5.4 Å, b ~ 23.2 Å, c ~ 21.2 Å, β ~ 95.2°; space group *C*2/*c*) (Fig. 1*b*).

2. Lobanovite sructure type in which Θ-ligands are absent (n = 0), and the neighboring *HOH* modules are combined by *A*-cations (a ~ 5.3 Å, b ~ 23.2 Å, c ~ 10.4 Å, β ~ 96.6°; space group *C*2/*m*) (Fig. 1*c*).

3. Sveinbergeite structure type in which Θ-ligands are present (n = 1), but the neighboring *HOH* modules are combined by *A*-cations (a ~ 5.3 Å, b ~ 11.8 Å, c ~ 11.8 Å, α ~ 101.1°, β ~ 98.2°, γ ~ 102.4°; space group $P\bar{1}$) (Fig. 1*d*).

Veblenite $K_2Na(Fe^{2+}_5Fe^{3+}_4Mn^{2+}_7\square)Nb_3Ti(Si_2O_7)_2(Si_8O_{22})_2O_6(OH)_{10}(H_2O)_3$ [21] is complex titanosilicate of the heterophillosilicate family whose *HOH* module is based on wide silicon-oxygen ribbons of the типа Si_8O_{22} veblenite type as well as Si_2O_7 diorthogroups (Fig. 2). Using $S_{N.n}$, we can write the general formula of the *HOH* module as follows [13, 21]:

$$(HOH)_{(Veb)} = \{^{[6]}M_{17}\varnothing_{10}[^{[6]}L_2O_2(Si_2O_7)(Si_8O_{22})\Theta^*]_2\},$$

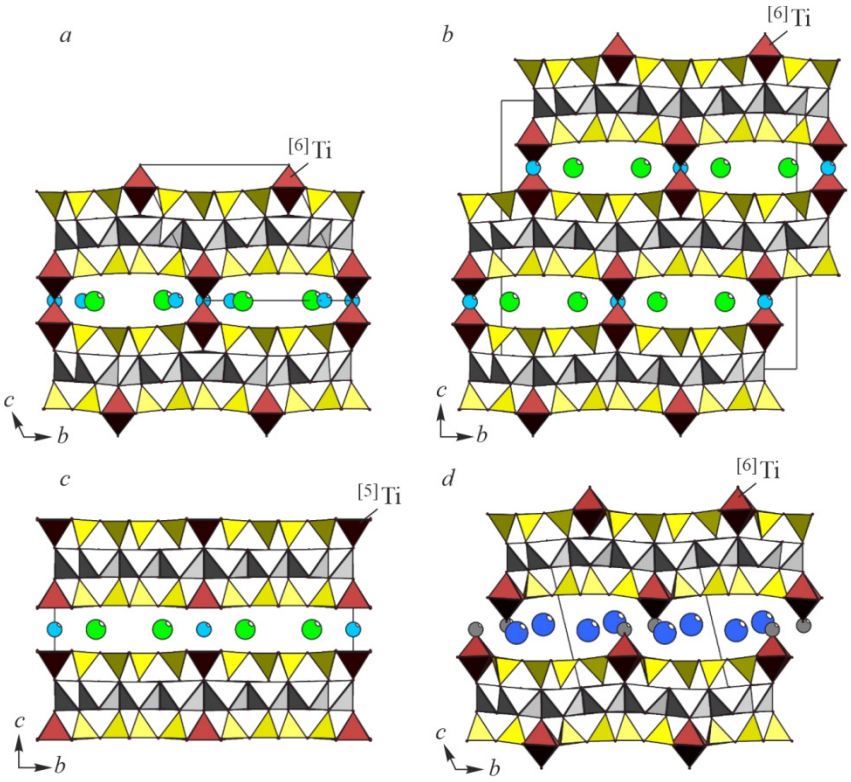

Fig. 1. General view of the crystal structure of astrophyllite group minerals: astrophyllite-1*A* (*a*), astrophyllite-2M (*b*), lobanovite (*c*), and sveinbergeite (*d*) (in the figure: MO_6 octahedra of the *O*-layer are shown by gray; SiO4 tetrahedra of the *H*-layer by yellow; light blue circles designate sodium; green are potassium; dark gray are calcium; large dark blue circles designate water molecules) (see el. version).

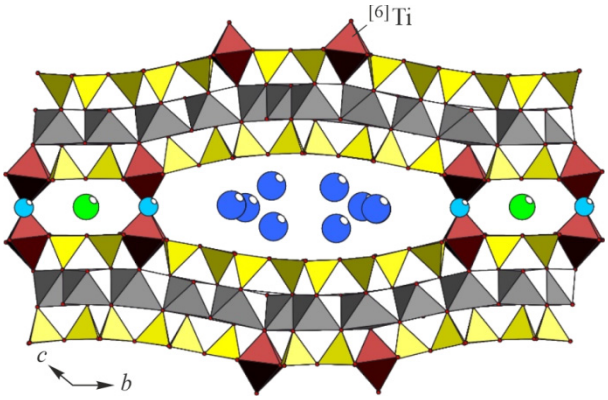

Fig. 2. Fragment of the veblenite crystal structure.

Owing to the presence of veblenite chains in the *H*-layer of the *HOH* module, the veblenite structure contains even wider channels than those in the nafertisite structure type [14].

It was shown previously that under supercritical conditions (in the temperature range of 400-600 °C and a pressure of 1000 kg/cm^2), astrophyllite exhibited ion exchange properties. In particular, under these conditions Na^+, Rb^+, and Cs^+ ions can substitute for K^+ ions [22, 23]. Under milder natural conditions, astrophyllite can be involved in ion exchange reactions with aqueous solutions, as a result of which, oxonium ions and water molecules substitute for Na^+ ions with the formation of so-called hydroastrophyllite $(H_3O,H_2O,K,Ca)_3(Fe,Mn)_{5\text{-}6}Ti_2Si_8(O,OH)_{31}$ [24], however, these processes take place over a long geological time. The ion exchange properties of lobanovite, sveinbergeite, and veblenite have not been studied

experimentally. Nonetheless, it is possible to assume that due to their crystal structures, ion exchange is unlimited because by analogy with micas and other clay minerals with layered structures [11, 25], the interlayer space can expand depending on the cation type (e.g., in devitoite, CO_3 and PO_4 groups are located in the interlayer space [26]).

The aim of this work was the theoretical analysis of possible migration paths of various cations (Na^+, K^+, Rb^+, Cs^+, Ag^+, Pb^{2+}, as the most common) in wide channels of framework representatives of the astrophyllite supergroup, as well as veblenite.

THEORETICAL CALCULATIONS

To analyze ion migration paths in astrophyllite group minerals using the ToposPro program package [27] we employed structure models of astrophyllite-1*A* [18], astrophyllite-2*M* [18], and veblenite [21]. This approach is based on the Voronoi–Dirichlet partition that makes it possible to obtain an adequate map of the system of cavities and channels [28]. The result of this partition is two interpenetrating graphs: atomic and void networks. The elementary void radius (R_{sd}) is calculated as a radius of the sphere whose volume equals the void volume of the Voronoi–Dirichlet polyhedron (VDP). By comparing the elementary void radius (R_{sd}) with the radius of a mobile atom in the respective environment [29, 30], it is possible to determine the probability of the atom location in this void. The elementary channel radius (R_{chan}) is calculated as the arithmetic mean of distances between the center of gravity of the elementary channel cross-section and atoms forming it. In estimating the channel radius, it is needed to multiply the sum of radii of the mobile cation and the atom forming the channel (oxygen) by the deformation coefficient γ [31] taking into account the possible polarization of ions during their passing through the channel [32-34].

Since not all voids and channels are significant (i.e., available for the migration of cations of a certain type), it is necessary to sort them out using the significance parameters found from VDP calculations of the known cation conductors. Table 1 lists the significance parameters for the void and channel radii if the migrating cation is Li^+, Na^+, K^+, Rb^+, Cs^+, Ag^+, or Pb^{2+}. Voids and channels having the radius smaller than the respective criteria together with channel systems were removed. A set of significant elementary voids and channels linking them forms the migration map describing all possible diffusion paths of the mobile cation [29, 30].

RESULTS AND DISCUSSION

Astrophyllite supergroup minerals with astrophyllite-1*A* and astrophyllite-2*M* structure types contain a system of wide parallel channels whose effective width (calculated as O···O distances determining the channel diameter minus 2.7 Å [35]) is 1.48×9.22 Å and is characterized by the 12-member cross-section (Fig. 3). According to recommendations of the International Zeolite Association and IUPAC, the crystal chemical formula of ordered microporous compounds can be

TABLE 1. Significance Parameters of Elementary Channels (R_{chan}) And voids (R_{sd}) Used to Construct Migration Maps

Working ion	R_{chan}, Å	R_{sd}, Å
Li^+	2.02	1.38
Na^+	2.16	1.54
Ag^+	2.20	1.58
Pb^{2+}	2.23	1.62
K	2.30	1.70
Rb^+	2.38	1.78
Cs^+	2.47	1.88

Note. In estimating channel sizes Slater's system of radii was used [29], and in estimating void radii the VDP radii for particular coordination spheres were used.

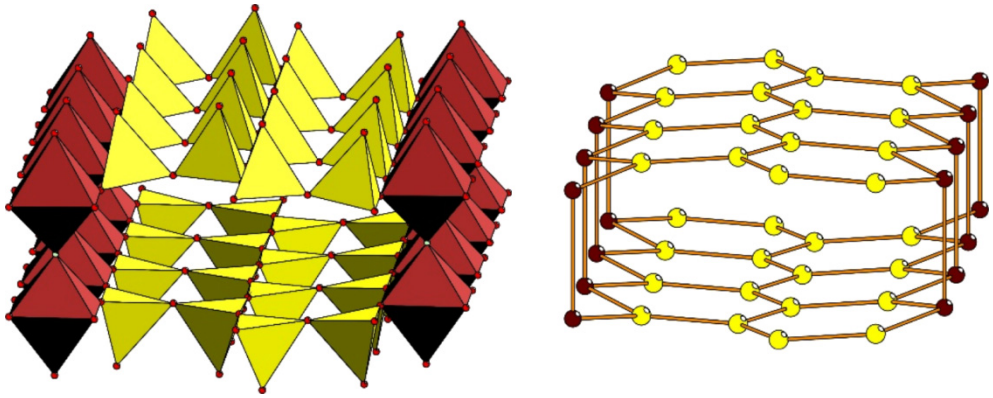

Fig. 3. Topology of the channels in the astrophyllite-1*A* and astrophyllite-2*M* types structure.

represented in the form [35, 36]: |guest composition| [host composition] $_h${host dimensionality} $_p${characteristic of pores/channels} (symmetry, space group). Thus, their crystal chemical formula should be written as (Z = 2)

$$|A_{2n}B_m(H_2O))_k|\ [^{[6]}M_7\varnothing_4[^{[6]}LO(Si_4O_{12})\Theta_n]_2]\ _h\{3\}\ _g\{1[6^612^{2/2}][100]\}\ (P\bar{1}\ \text{or}\ C2/c).$$

This formula reflects that the structures are based on *HOH* modules of the astrophyllite type, which combine and form a system of parallel channels directed along the *x* axis; guests of the structure are large *A*- and *B*-cations characterized by different charges and coordination numbers, as well as water molecules; n = 1, 2; m = 1, 2; k = 0-2.

By the topological analysis it is found that framework representatives of the astrophyllite supergroup, which correspond to astrophyllite-1*A* and astrophyllite-2*M* structure types, have one-dimensional conductivity channels of Na^+, K^+, Ag^+, Pb^{2+}, and Rb^+ ions along the [100] direction (Fig. 4*a*), whereas the Cs^+ ion is too large and cannot migrate along the channel. The centers of six-member rings of *H*-layers contain large voids linked with the central systems of channels suitable for the accommodation of large cations in the case of ion exchange in counter flows. As established previously for the nafertisite structure type [14], despite that a six-member window with the *B*-position in its center, which is occupied mainly by sodium, is present between the pairs of Tiφ_6 octahedra, the cation exchange between the neighboring channels does not occur through it because of a number of steric hindrances related, first of all, to its effective sizes.

The ion conductivity changes from one-dimensional to two-dimensional when Li^+ ions are used: owing to the small radius, they can migrate between the neighboring channels through the *B*-position in astrophyllite-1*A* and astrophyllite 2*M* structure types (Fig. 4*b*), similarly to the nafertisite structure type [14]. As in the case of large cations, the six-member rings of *H*-layers contain voids suitable for Li^+ ions linked with the central conductive layer and can be occupied during the ion exchange in countercurrent flows.

The veblenite crystal structure has two types of channels: narrow and wide with cross-sections having effective sizes of 0.9×5.0 Å (hexagonal) and 4.1×17.2 Å (icosagonal), respectively (Fig. 5). The crystal chemical formula of veblenite can be written as (Z = 2)

$$|A_3B_2(H_2O)_k|\ [M_{17}\varnothing_{10}[^{[6]}L_2O_2(Si_2O_7)(Si_8O_{22})\Theta^*]_2]\ _h\{3\}\ _p\{1[6^{10}20^{2/2}][100]/1[6^{4/2}][100]\}(P\bar{1}),$$

where A = K, □; B = Na, □.

Due to the presence of tetrahedral ribbons of the veblenite type in the *H*-layer, the veblenite crystal structure contains the widest channels known at present among the representatives of the heterophyllosilicate family. In the narrow channel, the migration of ions with a sufficiently small radius, e.g. Na^+, is also possible. With an increase in the ion radius its width becomes insufficient, and already for the Ag^+ ion there are only separate voids within the channel that can accommodate it. For Pb^{2+} and cations with a larger ionoc radius the narrow channel is completely excluded from the conductive system. Effective sizes of the wide channel in the veblenite structure provide the ion exchange for all ions in counter flows, including large Cs^+. For Li^+ ions the conductivity becomes two-dimensional due to the possible migration of ions through the respective windows between the neighboring channels (similarly to the astrophyllite and nafertisite structure types).

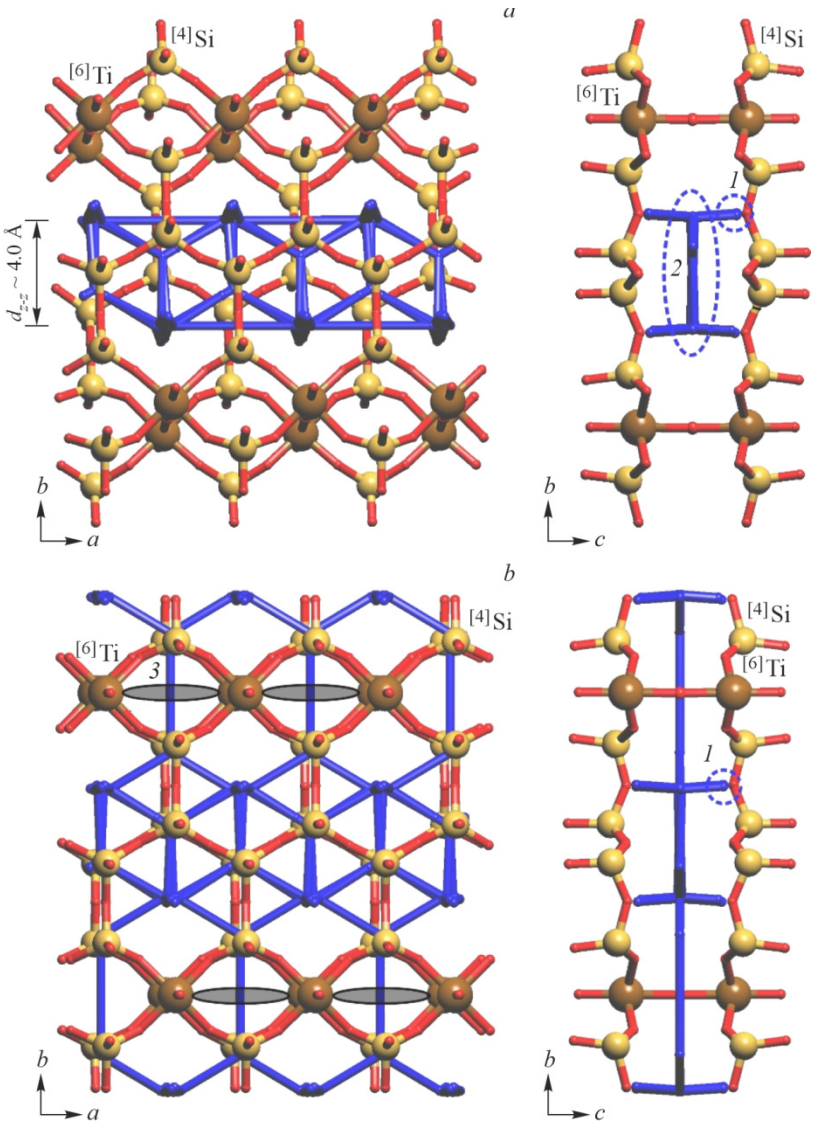

Fig. 4. Migration paths of Na, Ag, Pb, K, Rb (*a*) and Li (*b*) cations in the astrophyllite-1*A*/-2*M* structure type: *1* - additional voids in the centers of six-member rings of *H*-layer; *2* - main conductivity channel; *3* - windows between the neighboring channels.

A comparative characteristic of the migration paths for different cations in titanosilicates of the heterophyllosilicate family is presented in Table 2.

CONCLUSIONS

By topological calculations it is found that in heterophyllosilicates with astrophyllite-1*A*/-2*M* and veblenite structure types, the one-dimensional character of the ion conductivity of alkali metals (Na^+, K^+, Rb^+, Cs^+), silver (Ag^+), and lead (Pb^{2+}) can occur through the system of wide parallel channels in the [100] direction. The neighboring channels are separated by walls of connected $Ti\varphi_6$ octahedra from *H*-layers, which hinder the cation exchange between the channels. Lithium substitution for large alkali cations substantially changes the character of the cation conductivity. Owing to the smaller radius, Li^+ ions can pass through the window between the channels, forming a two-dimensional conductive layer parallel to (001). For purely layered structures similar to micas and clay materials it may be assumed that the ion exchange as well as the

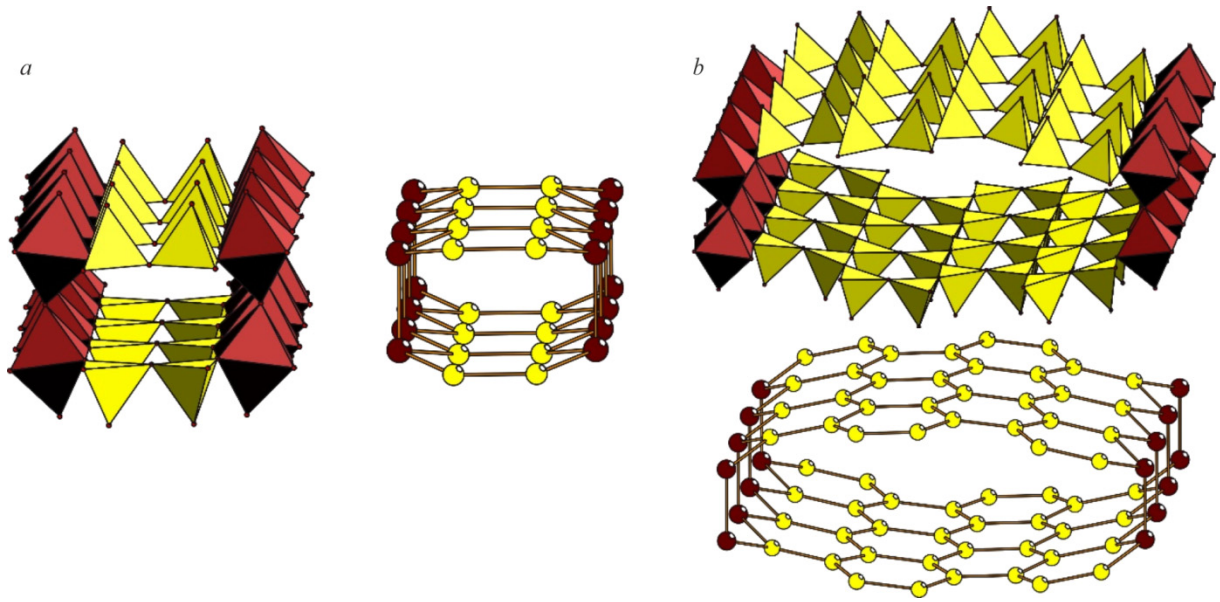

Fig. 5. Two types of channels in the structure of veblenite crystal: narrow (*a*) and wide (*b*).

TABLE 2. Comparative Characteristics of Channels in Heterophyllosilicates

Structure type / *HOH* module	Channel topology	Effective width, Å	Conductivity character						
			Li^+	Na^+	Ag^+	Pb^{2+}	K^+	Rb^+	Cs^+
Astrophyllite-1*A*/-2*M* $\{M_7\varnothing_6[^{[6]}LO(Si_4O_{12})\Theta_{0.5}]_2\}$	$\{1[6^6 12^{2/2}][100]\}$	1.5×9.2	2D	1D	1D	1D	1D	1D	-
Nafertisite $\{M_{10}\varnothing_6[^{[6]}LO(Si_6O_{17})\Theta_{0.5}]_2\}$	$\{1[6^8 16^{2/2}][100]\}$	2.2×13.5	2D	1D	1D	1D	1D	1D	1D
Veblenite $\{M_{17}\varnothing_{10}[^{[6]}L_2O_2(Si_2O_7)(Si_8O_{22})\Theta^*]_2\}$	$\{1[6^{4/2}][100]\}$ $\{1[6^{10}20^{2/2}][100]\}$	0.9×5.0 4.1×17.2	2D	1D 1D	0D 1D	- 1D	- 1D	- 1D	- 1D

sorption capacity are unlimited because the interlayer space can expand depending on the ion type and/or the respective cation or anion group, and also a neutral molecule.

FUNDING

The work was supported by the Russian Science Foundation, grant No. 20-77-10065 (theoretical topological analysis of migration paths).

CONFLICT OF INTERESTS

The authors declare that they have no conflict of interests.

REFERENCES

1. N. V. Chukanov, I. V. Pekov, and R. K. Rastsvetaeva. *Russ. Chem. Rev.*, **2004**, *73*, 205. https://doi.org/10.1070/RC2004v073n03ABEH000825
2. K. Popa and C. C. Pavel. *Desalination*, **2012**, *293*, 78. https://doi.org/10.1016/j.desal.2012.02.027
3. J. Rocha and Z. Lin. *Rev. Mineral. Geochem.*, **2005**, *57*, 173. https://doi.org/10.2138/rmg.2005.57.6

4. J. Rocha and M. W. Anderson. *Eur. J. Inorg. Chem.*, **2000**, *2000*, 801. https://doi.org/10.1002/(SICI)1099-0682(200005)2000:5%3C801::AID-EJIC801%3E3.0.CO;2-E
5. S. M. Kuznicki, V. A. Bell, S. Nair, H. W. Hillhouse, R. M. Jacubinas, C. M. Braunbarth, B. H. Toby, and M. Tsapatsis. *Nature*, **2001**, *412*, 720. https://doi.org/10.1038/35089052
6. Z. Lin, F. A. A. Paz, and J. Rocha. In: Layered Mineral Structures and their Application in Advanced Technologies / Eds. M. F. Brigatti and A. Mottana. Mineralogical Society of Great Britain and Ireland, **2011**, 123. https://doi.org/10.1180/EMU-notes.11.3
7. G. Ferraris, A. Bloise, and M. Cadoni. *Microporous Mesoporous Mater.*, **2008**, *107*, 108. https://doi.org/10.1016/j.micromeso.2007.02.036
8. I. S. Lykova, N. V. Chukanov, A. I. Kazakov, V. P. Tarasov, I. V. Pekov, V. O. Yapaskurt, and N. A. Chervonnaya. *Phys. Chem. Mineral.*, **2013**, *40*, 625. https://doi.org/10.1007/s00269-013-0598-0
9. I. S. Lykova, I. V. Pekov, N. V. Zubkova, N. V. Chukanov, V. O. Yapaskurt, N. A. Chervonnaya, and A. A. Zolotarev. *Eur. J. Mineral.*, **2015**, *27*, 535. https://doi.org/10.1127/ejm/2015/0027-2445
10. A. Zagorodni. Ion Exchange Materials: Properties and Applications. Elsevier, **2006**. https://doi.org/10.1016/B978-008044552-6/50006-X
11. G. Ferraris and A. Gula. *Rev. Mineral. Geochem.*, **2005**, *57*, 69. https://doi.org/10.2138/rmg.2005.57.3
12. R. K. Rastsvetaeva and S. M. Aksenov. *Crystallogr. Rep.*, **2011**, *56*. https://doi.org/10.1134/S1063774511060216
13. F. C. Hawthorne. *Mineral. Mag.*, **2012**, *76*, 1053. https://doi.org/10.1180/minmag.2012.076.5.13
14. N. V. Chukanov, S. M. Aksenov, I. V. Pekov, N. A.Chervonnaya, D. A.Varlamova, V. N. Ermolaeva, and S. N. Britvin. *Microporous Mesoporous Mater.*, **2021**, *312*, 110776. https://doi.org/10.1016/j.micromeso.2020.110776
15. E. Sokolova, F. Cámara, F. C. Hawthorne, and M. E. Ciriotti. *Mineral. Mag.*, **2017**, *81*, 143. https://doi.org/10.1180/minmag.2016.080.077
16. P. C. Piilonen, A.r.E. Lalonde, A. M. McDonald, R. A. Gault, and A. O. Larsen. *Can. Mineral.*, **2003**, *41*, 1. https://doi.org/10.2113/gscanmin.41.1.1
17. N. A. Yamnova and S. M. Aksenov. *Crystallogr. Rep.*, **2021**, *66*(7), 1167. https:// doi.org/10.1134/S1063774521070210
18. P. C. Piilonen, A. M. McDonald, and A. E. Lalonde. *Can. Mineral.*, **2003**, *41*, 27. https://doi.org/10.2113/gscanmin.41.1.27
19. E. Sokolova. *Mineral. Mag.*, **2012**, *76*, 863. https://doi.org/10.1180/minmag.2012.076.4.04
20. P. C. Piilonen, A. M. McDonald, and A. E. Lalonde. *Eur. J. Mineral.*, **2001**, *13*, 973. https://doi.org/10.1127/0935-1221/2001/0013/0973
21. F. Cámara, E. Sokolova, F. C. Hawthorne, R. Rowe, J. D. Grice, and K. T. Tait. *Mineral. Mag.*, **2013**, *77*, 2955. https://doi.org/10.1180/minmag.2013.077.7.06
22. N. F. Chelishchev. *Geokhimiya*, **1972**, *7*, 856.
23. N. F. Chelishchev. Ionoobmennye svoistva mineralov (Ion Exchange Properties of Minerals). Nauka, **1973**. [In Russian]
24. X-ray Laboratory. Hubei (Hupei) Geologic College. *Sci. Geol. Sin.*, **1974**, *1*, 18.
25. P. Cool, E. F. Vansant, G. Poncelet, and R. A. Schoonheydt. In: Handbook of Porous Solids / Eds. F. Schüth, K. S. W. Sing, and J. Weitkamp. Wiley-VCH Verlag GmbH, **2002**, 1250.
26. A. R. Kampf, G. R. Rossman, and I. M. Steele. *Can. Mineral.*, **2010**, *48*, 29. https://doi.org/10.3749/canmin.48.1.29
27. V. A. Blatov, A. P. Shevchenko, and D. M. Proserpio. *Cryst. Growth Des.*, **2014**, *14*, 3576. https://doi.org/10.1021/cg500498k
28. N. A. Anurova and V. A. Blatov. *Acta Crystallogr.*, *Sect. B: Struct. Sci.*, **2009**, *65*, 426. https://doi.org/10.1107/S0108768109019880
29. V. A. Blatov, G. D. Ilyushin, O. A. Blatova, N. A. Anurova, A. K. Ivanov-Schits, and L. N. Dem′yanets. *Acta Crystallogr.*, *Sect. B: Struct. Sci.*, **2006**, *62*, 1010. https://doi.org/10.1107/S0108768106039425

30. V. A. Blatov and A. P. Shevchenko. *Acta Crystallogr*., *Sect. A: Found. Crystallogr.*, **2003**, *59*, 34.
31. V. I. Voronin, M. G. Surkova, G. S. Shekhtman, N. A. Anurova, and V. A. Blatov. *Inorg* Mater., **2010**, *46*, 1234-1241. https://doi.org/10.1134/S0020168510110130.
32. N. A. Anurova and V. A. Blatov. *Neorg. Mater.*, **2010**, *46*, 1360. [In Russian]
33. S. S. Fedotov, N. A. Kabanova, A. A. Kabanov, V. A. Blatov, N. R. Khasanova, and E. V. Antipov. *Solid State Ionics*, **2018**, *314*, 129-140. https://doi.org/10.1016/j.ssi.2017.11.008
34. R. A. Eremin, N. A. Kabanova, Y. A. Morkhova, A. A. Golov, and V. A. Blatov. *Solid State Ionics*, **2018**, *326*, 188. https://doi.org/10.1016/j.ssi.2018.10.009
35. L. B. McCusker, F. Liebau, and G. Engelhardt. *Microporous Mesoporous Mater.*, **2003**, *58*, 3. https://doi.org/10.1016/S1387-1811(02)00545-0
36. F. Liebau. *Microporous Mesoporous Mater.*, **2003**, *58*, 15. https://doi.org/10.1016/S1387-1811(02)00546-2